Wireless Power Transfer Using Weakly Coupled Magnetostatic Resonators

José Oscar Mur-Miranda, Giulia Fanti, Yifei Feng, Keerthik Omanakuttan, Roydan Ongie, Albert Setjoadi and Natalie Sharpe
Franklin W. Olin College of Engineering, Needham, Massachusetts 02492

***Abstract*—Wireless power transfer can create the illusion of portable devices with infinite power supplies and enable applications that are currently unimaginable because of power constraints. Magnetic induction has been extensively used for wireless power transfer, but its efficiency depends on magnetic coupling that decays as the inverse cube of distance. At long enough distances, the magnetic coupling is weak enough that the effect of the receiver coil on the sender coil can be neglected. In this weakly coupled limit, series resonance in both the sender and the receiver increases the power transfer. Compared to magnetic induction, the power transfer increases by the sum of the quality factors of the sender and the receiver times the quality factor of the sender. Similarly, the efficiency increases by half of the product of the quality factors of the sender and the receiver. However, the overall efficiency of the power transfer is less than 50% for all weakly coupled series resonators. Resonators with a Q of 1,000 should be able to send power over a distance 9 times the radius of the devices with an efficiency of 10%.**

***Index Terms*—wireless power transfer, magnetic resonance, coupled resonators, ambient power**

I. Motivation

PORTABLE devices are still constrained to the use of batteries or some other form of energy storage. Even with advances in the reduction of power consumption, batteries typically are the largest and heaviest component in modern portable devices. Wireless power transfer can enable the creation of *ambient power*, where devices send and receive power to each other. Applications include sensor networks, wearable computing, and implanted medical devices. For instance, sensors and actuators in a robotic arm or in rotating machinery should benefit from wireless power distribution since cables could become tangled. Cables might also impede the motion of people around electrical equipment or be an added cost in terms of weight and price, such as in an improvised operating room in an isolated location or a battlefield. In these cases, wireless electric power transfer in the range of a few feet is an ideal solution. On the other hand, wireless power transfer could also be useful in applications where power is extracted from energy harvesters whose placement may be constrained. For example, a vibration energy harvester might need to be attached to the rotor of a motor, while the load might need to be attached to the stator. Similarly, electromagnetic radiation harvesters are sometimes located in places where the circuitry of the load cannot survive. The need for ambient power in these and other applications is likely to increase as portable, distributed, low power systems become more common.

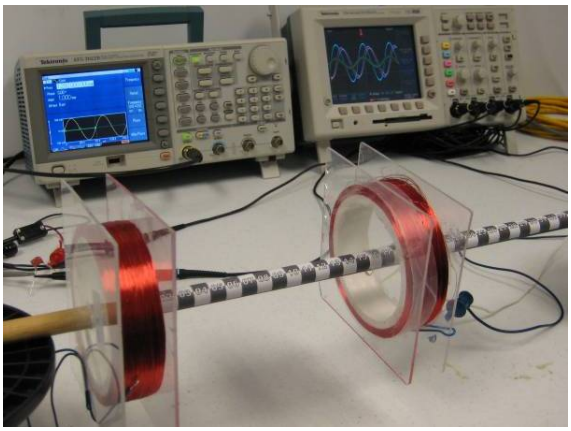

Fig. 1. Wireless power transfer system. The air core coils were kept aligned axially. The sender coil was made using about 2,400 turns of 32 AWG copper wire and has an inner radius of 4.5 cm and an outer radius of 5.0 cm, a length of 2.5 cm, an inductance of $L_1 = 740$ mH, a series resistance of $R_{L_1} = 395\ \Omega$ and a parasitic capacitance of $C_{L_1} = 236$ pF. The receiver coil was made using the same number of turns, wire and dimensions, but fabrication errors yield an inductance of $L_2 = 745$ mH, a series resistance of $R_{L_2} = 395\ \Omega$ and a parasitic capacitance of $C_{L_2} = 240$ pF.

II. Scope

The model in this paper quantifies the improvement in power transfer and efficiency obtained by adding resonance to weak magnetic coupling. The resulting expressions illustrate the performance bounds of wireless power transfer using resonant magnetic coupling and are useful in the design of wireless power transfer systems. These results are validated with the experimental setup shown in Figure 1.

The system implementation explored in this paper is a coil connected in series to a capacitor which acts as a resonator. One resonator is connected to a voltage source and functions as the power sender while the other resonator is connected to a load and acts as power receiver, as shown in Figure 2. A model consisting of a pair of magnetically coupled series RLC circuits captures the improvement in power transfer due to coupled magnetic resonance. This model is solved analytically when the separation distance is several times larger than the device size and the magnetic coupling is so weak that the impedance presented by the receiver coil to the sender coil is negligible.

The power transferred with magnetic inductive coupling without resonance is limited by the large self impedances of L_1 and L_2 in comparison to the mutual impedance of L_M. This

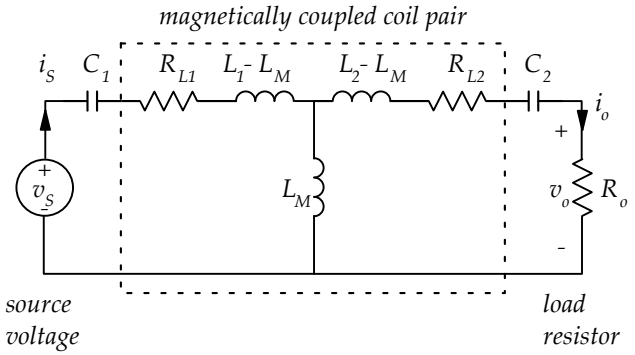

Fig. 2. Circuit model for wireless power transfer using magnetically coupled resonators. The mutual inductance $L_M = \kappa\sqrt{L_1 L_2}$, where $0 < \kappa < 1$.

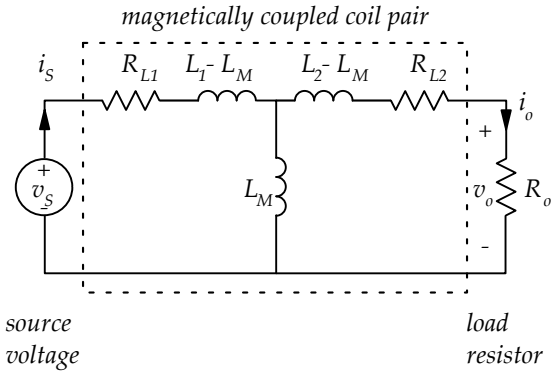

Fig. 3. Equivalent model for inductive coupling. The mutual inductance $L_M = \kappa\sqrt{L_1 L_2}$, where $0 < \kappa < 1$.

is inevitable since $L_M \ll L_1, L_2$ when the coils are separated more than a few times their size. However, the impedances of L_1 and L_2 can be eliminated by adding a capacitor in series with each inductor, as shown in Figure 2, and tuning each capacitor to resonate with its respective inductor at the same frequency. This topology is not necessarily optimal but should be broad enough to encompass systems with other topologies. Furthermore, the magnetic coupling between the coils depends on their relative orientation, separation distance and geometry. However, the model only captures the effect of the separation distance on the magnetic coupling and ignores other variables. While more detailed models will yield more accurate results, the validation shows that the added complexity is not necessary. The results from this analysis can be used to estimate the performance of wireless power transfer systems based on dimensions and component characteristics.

III. Background

Tesla patented wireless power transfer using resonant coupling at the turn of the last century [1]. However, it is unclear if he succeeded in sending power. The devices in his patent are several meters high and could conceivably send power quantities close to the megawatt range. Given the recent interest in wireless power transfer, many research groups and companies are currently analyzing and developing power transfer systems that rely on resonant magnetic coupling. Several systems have been studied that use either resonant senders or receivers [2], [3], but the first demonstration of wireless power transfer using resonance on both ends was published in 2007 [4], [5]. The resonators in this experiment were identical coils and achieved 30% real power efficiency at 10 MHz over a distance 7.5 times the radius of the sending and receiving coils. The prediction of the resonant frequency has a 5% error and the estimated quality factor Q is 2.6 times larger than the measurement. The authors modeled the system using coupled mode theory (CMT), which is more general and abstract than the lumped element model of a series RLC topology used in this paper. Their analysis is expressed within the context of the model in this paper in order to compare their results.

In [6], the application of a well understood model for inductive coupling serves to verify that resonance improves the efficiency of wireless power transfer, but this model is not useful for detailed system design. A lumped element model introduced in [7], [8] may facilitate the design of similar systems, but it is not clear why the source capacitor is placed in series with the source inductance. Also, it is unclear why the load resistance is only assumed to be large and is not included in the optimization. Their experimental system demonstrates a 23 W transfer at 1.4 times the size of the device but does not provide a measurement of efficiency. In both cases, the authors provide a theoretical model that validates their measurements, but they don't provide algebraic expressions for efficiency and power transferred.

Sony Corporation has announced a product based on magnetic resonance capable of sending power with 80% efficiency over 50 cm, but do not specify the dimensions of the sender or receiver [9]. Intel Corporation has also announced that it is exploring this technology but has not provided any details [10].

IV. Magnetic coupling without resonance

The circuit shown in Figure 3 models a system of two magnetically coupled coils sending power from a voltage source v_S to a load resistance R_o. This system is impractical for wireless power transfer at long distances since the efficiency drops to 0.1% at a distance equal to the diameter of the coils. However, the result provides a baseline to quantitatively measure the improvement offered by resonant coupling. The inductance L_1 is the self inductance of the sender coil, which is only physically connected to the voltage source v_S. The inductance L_2 represents the self inductance of the receiver coil, which is only physically connected to the load resistor R_o. The inductance L_M represents the mutual inductance between the two coils, which is purely a function of the geometry of the solenoids and is independent of the current or voltage through the inductors [11, p. 294]. The mutual inductance is bounded such that $L_M \leq \sqrt{L_1 L_2}$. The magnetic coupling coefficient κ is defined as

$$\kappa \stackrel{\text{def}}{=} \frac{L_M}{\sqrt{L_1 L_2}}, \tag{1}$$

such that $0 \leq \kappa \leq 1$.

If the coils are sufficiently far apart compared to their dimensions, the details of their geometry will be irrelevant. Therefore, the magnetic coupling coefficient of ideal spherical inductors, also known as "flux balls," [12, pp. 30-33] is

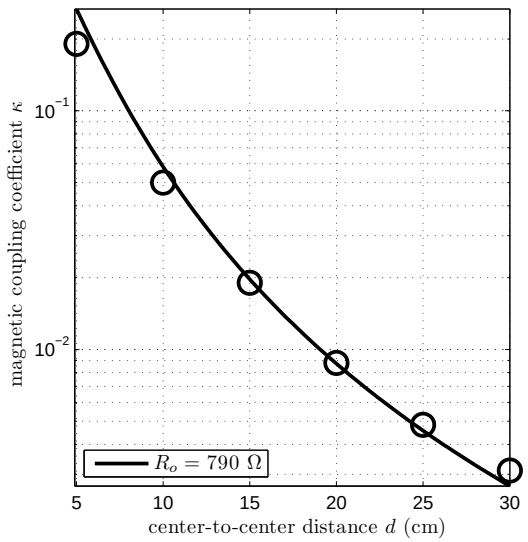

Fig. 4. Magnetic coupling coefficient (κ) for the system described in Figure 1. The measurements were made using an output resistor $R_o = 790\ \Omega$.

approximately equal to the magnetic coupling coefficient of any other system when the distance d between them is much larger than their respective radii r_1 and r_2. In this case, the magnetic coupling coefficient κ is approximately equal to

$$\kappa \approx \frac{1}{2(d/\sqrt{r_1 r_2})^3}, d \gg r_1, d \gg r_2. \tag{2}$$

The experimental setup shown in Figure 1 fits this model by adjusting the effective radius of the coils to $r_1 = r_2 = 5.3$ cm and including the effect of the coil geometry as the distance d becomes comparable to the coil dimensions,

$$\kappa = \frac{1}{[1 + 2^{2/3}(d/\sqrt{r_1 r_2})^2]^{3/2}}, \tag{3}$$

as shown in Figure 4. Note that $\kappa < 1/16$ for distances greater than twice the radius of the coils and decreases as $1/d^3$.

Assuming $\kappa \ll 1$, the real power output $P_o = \Re\{V_o I_o^*/2\}$ delivered to R_o is maximized when

$$f_{max} = \frac{1}{2\pi}\sqrt{\frac{R_{L_1}}{L_1}\left(\frac{R_{L_1}}{L_1} + 2\frac{R_{L_2}}{L_2}\right)} \tag{4}$$

and

$$R_{o,max} = R_{L_1}\frac{L_2}{L_1} + R_{L_2}. \tag{5}$$

The details of this derivation are in Appendix A. The power output under this condition is

$$\begin{aligned} P_{o,max} &= \left.\frac{|V_o|^2}{2R_{o,max}}\right|_{f=f_{max}, R_o = R_{o,max}} \\ &= \frac{|V_s|^2}{4R_{L_1}}\frac{\kappa^2}{2}\frac{1}{1 + \frac{R_{L_2}/L_2}{R_{L_1}/L_1}}. \end{aligned} \tag{6}$$

Figure 5 shows the power output as a function of distance for the setup shown in Figure 1. The real power efficiency

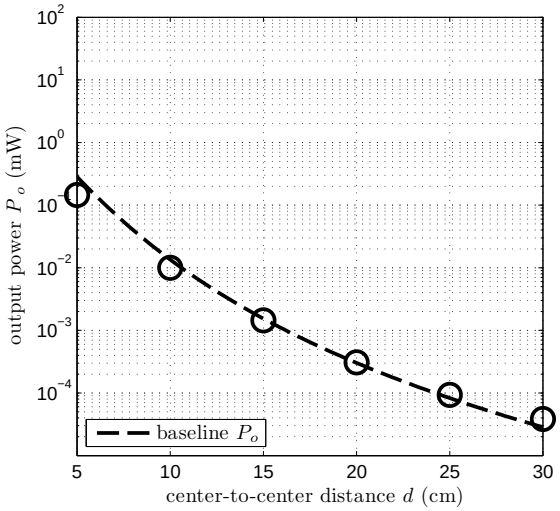

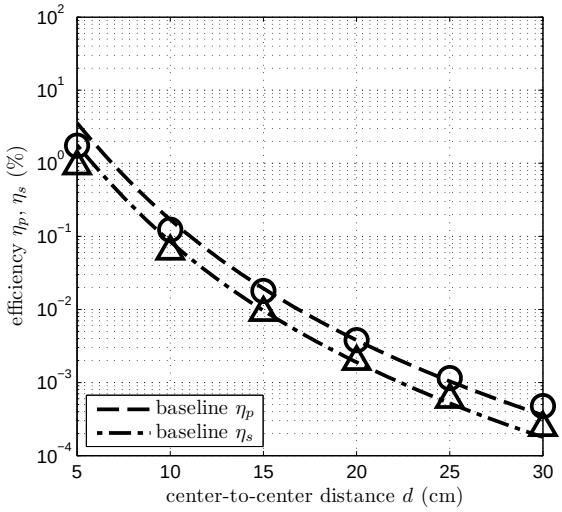

Fig. 5. Power transferred and efficiency as a function of distance for two air core coils where the sender is driven with a sinusoid of amplitude $V_s = 5$ V at $f_{max} = 147$ Hz. The sender and receiving coils are the same as described in Figure 1. The output resistance was set to the theoretical $R_{o,max} = 790\ \Omega$. The efficiencies η_p and η_s are normalized with respect to the real power and the apparent power sent by the source, respectively.

$\eta_p \stackrel{\text{def}}{=} P_o/P_s$ is

$$\eta_p = \frac{P_o}{|V_s||I_s|\cos(\angle Z_s)} = \frac{\kappa^2}{2}, \tag{7}$$

where $Z_s = V_s/I_s$. Since this input impedance is not purely real, the complex power $S_s = V_s I_s^*/2 = P_s + jQ_s$ delivered by the source has nonzero real and reactive parts. The apparent power efficiency $\eta_s \stackrel{\text{def}}{=} P_o/|S_s|$ includes the total magnitude of the complex power in order to take this into account. For this system,

$$\eta_s = \frac{P_o}{|V_s||I_s|} = \frac{\kappa^2}{2}\frac{1}{\sqrt{2}\sqrt{1 + \frac{R_{L_2}/L_2}{R_{L_1}/L_1}}}. \tag{8}$$

Appendix A shows that $\eta_s \leq \eta_p/\sqrt{2}$, and $\eta_s = \eta_p/2$ if the sender and receiver coils are identical.

V. Resonant inductive coupling

In the circuit shown in Figure 2, the impedance of the receiver couples to the source through the magnetic coupling represented by L_M. When the separation distance becomes large enough, the magnetic coupling becomes so weak that the impedance presented by the receiver to the source becomes negligible. In this case, the magnetic coupling coefficient κ must fulfill the condition

$$\kappa^2 \ll \frac{1}{1-\eta_{max,res}} \cdot \frac{1}{Q_1 Q_2}, \tag{9}$$

where Q_1 and Q_2 are the quality factors of the sender and receiver resonators,

$$Q_1 \stackrel{\text{def}}{=} \frac{\sqrt{L_1/C_1}}{R_{L_1}} \qquad Q_2 \stackrel{\text{def}}{=} \frac{\sqrt{L_2/C_2}}{R_{L_2}}, \tag{10}$$

and $\eta_{max,res}$ is the ideal maximum efficiency that the system can achieve at resonance,

$$\eta_{max,res} = \frac{R_o}{R_o + R_{L_2}}. \tag{11}$$

The power output is maximized when the circuit is driven at resonance. The details of this derivation are in Appendix B. The maximum power transferred is

$$P_{o,max,res} = \frac{|V_s|^2}{2R_{L_1}} \frac{\kappa^2}{2} \frac{Q_1 Q_2}{2}. \tag{12}$$

The power output with resonant magnetic coupling is larger than the power output in the baseline system by a factor of

$$\frac{P_{o,max,res}}{P_{o,max}} = Q_1^2 + Q_1 Q_2. \tag{13}$$

Figure 6 shows the maximum power and efficiency in a resonant system created by adding 20 nF capacitors to the coils described in Figure 1. The quality factors Q_1 and Q_2 are equal to 15. Substitution of these values into the expression above shows that the power output in the resonant case is 470 times larger.

Since the impedance is purely real at resonance, both the apparent and real efficiencies are

$$\eta_{p,res} = \eta_{s,res} = \frac{\kappa^2}{2} \frac{Q_1 Q_2}{2}. \tag{14}$$

The efficiency using resonance is

$$\frac{\eta_{p,res}}{\eta_p} = \frac{Q_1 Q_2}{2} \tag{15}$$

times higher than the real efficiency η_p in the system without resonance. The real efficiency of the system measured in Figure 6 is 120 times larger than the real efficiency of the baseline system. This improvement is approximated in [4] to $(2Q_2)^2$, which is 8 times larger than Equation 15 if the sender and receiver are identical.

If a system is operating at a distance such that it is weakly coupled and Equation 9 is satisfied, then the efficiency is bounded such that $\eta_{p,res} \ll \eta_{max,res}$ for any value of R_o. Furthermore, if the output resistance $R_o = R_{L_2}$ in order

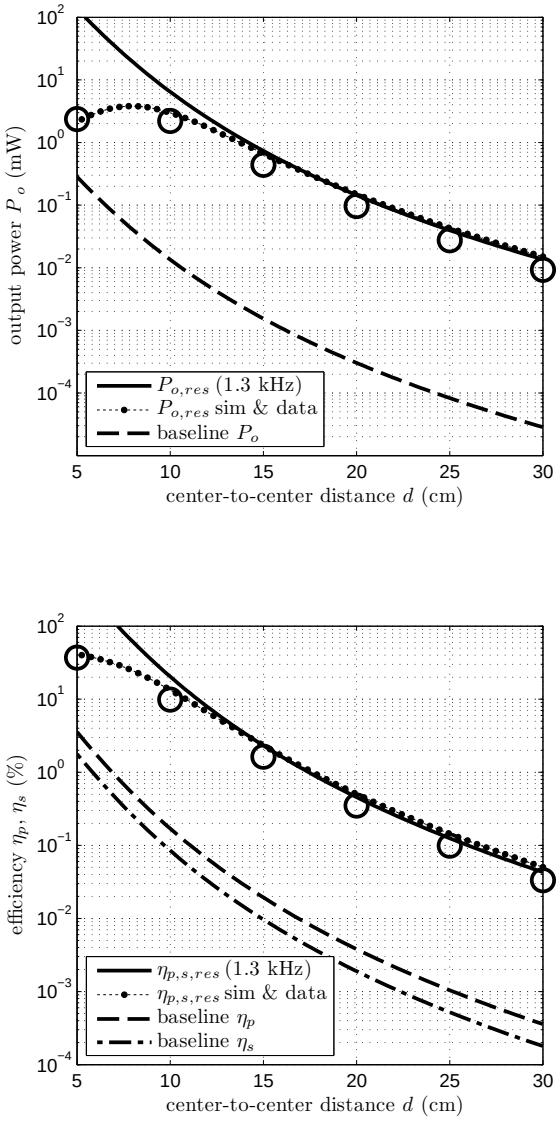

Fig. 6. Power transferred and efficiency as a function of distance for two resonators made with the coils described in Figure 1 and resonating capacitors $C_1 = C_2 = 20$ nF. The source coil was driven with a sinusoid of amplitude $V_s = 5$ V at the resonant frequency $f_{max,res} = 1.3$ kHz. The output resistance was set to $R_{o,max,res} = 395\ \Omega$. The measurement data is bounded by the expressions for power and efficiency derived from the baseline model without resonant coupling in Figure 5, as well as compared to a simulation of the resonant model that includes the parasitic capacitances of the coils as shown in Figure 7 and discussed in Section VI. The efficiencies η_p and η_s are normalized with respect to the real power and the apparent power sent by the source, respectively.

to maximize the power delivered and the efficiency, then $\eta_{max,res} = 1/2$ and $\eta_{p,res} \ll 1/2$. Since

$$P_{o,max,res} = \frac{|V_s|^2}{2R_{L_1}} \eta_{p,res}, \tag{16}$$

then

$$P_{o,max,res} \ll \frac{|V_s|^2}{2R_{L_1}} \cdot \frac{1}{2}. \tag{17}$$

In addition, the condition for weak coupling where this

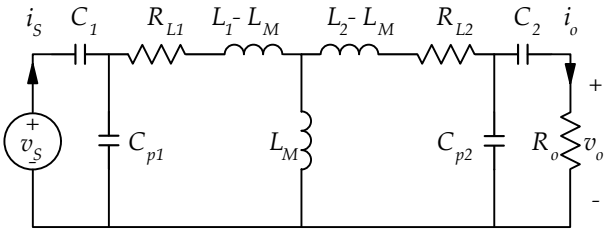

Fig. 7. Equivalent model for a coupled LC resonator including parasitic capacitance of the coils.

model is valid, Equation 9, becomes

$$\kappa^2 \ll \frac{2}{Q_1 Q_2}. \tag{18}$$

In comparison, the condition for strong coupling in [4] is

$$\kappa^2 > \frac{1}{Q_1 Q_2}. \tag{19}$$

where "strong coupling" is defined within the context of coupled mode theory. Their coupling coefficient is based on CMT, and is different from the magnetic coupling coefficient κ. In particular,

$$\kappa_{CMT} = \frac{\omega}{2}\frac{L_M}{\sqrt{L_1 L_2}} = \frac{\omega}{2}\kappa, \tag{20}$$

where ω is the frequency of the resonant mode. Furthermore, κ_{CMT} is not defined for a system without resonance.

The expression for maximum power $P_{o,max,res}$ suggests that performance improves if the resonating capacitors C_1 and C_2 are minimized for any given coil. The next two sections detail the principal problems with the model as these capacitors are minimized and the resonant frequency is increased.

VI. Parasitic capacitance limitations

Figure 8 shows the power transferred and efficiency as a function of distance for two resonators where the resonating capacitances C_1 and C_2 are equal to 2 nF, which is comparable to the parasitic capacitances $C_{p_1} = 236$ pF and $C_{p_2} = 240$ pF present in the coils, as shown in Figure 7. Note that the measured power output is less than the model prediction. Introduction of the parasitic capacitances into the original model accounts for the observed difference. Figure 6 also shows the results of a simulation that includes the parasitic capacitances in the model, but, as expected, the effect is negligible when compared to the 20 nF resonating capacitors.

VII. Core loss limitations

Inductors with ferrite cores have larger inductances than similar inductors with air cores. However, the core losses are larger with a ferrite core. The effect of core losses may be represented as a resistance in parallel with the inductance as shown in Figure 9. Figure 10 shows the power transferred and efficiency as a function of distance for two ferrite core coils. The system is compared to a simulation of an identical system without any core losses. Introduction of the core losses into the original model accounts for the difference between the power output predicted and the power output measured.

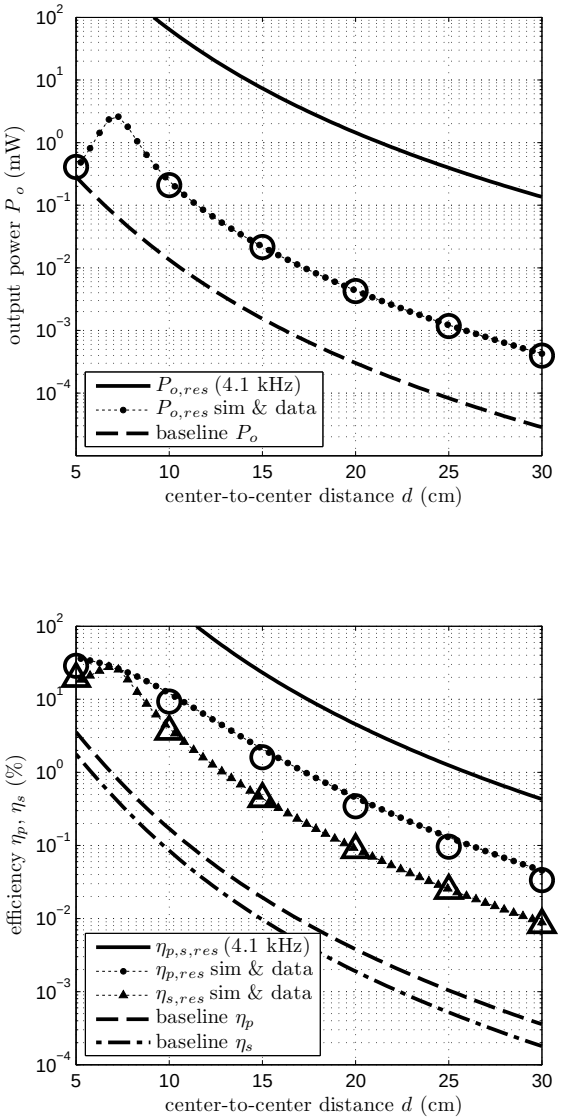

Fig. 8. Power transferred and efficiency as a function of distance for two resonators made with the coils described in Figure 1, resonating capacitors $C_1 = C_2 = 2.0$ nF, and driven with a sinusoid of amplitude $V_s = 5$ V at the resonant frequency $f_{max,res} = 4.1$ kHz. The output resistance was set to $R_{o,max,res} = 395\ \Omega$. The measurement data is bounded by the expressions for power and efficiency derived from the resonant model at 4.1 kHz and the baseline model without resonant coupling in Figure 5, as well as compared to a simulation of the resonant model that includes the parasitic capacitances of the coils as shown in Figure 7. The efficiencies η_p and η_s are normalized with respect to the real power and the apparent power sent by the source, respectively.

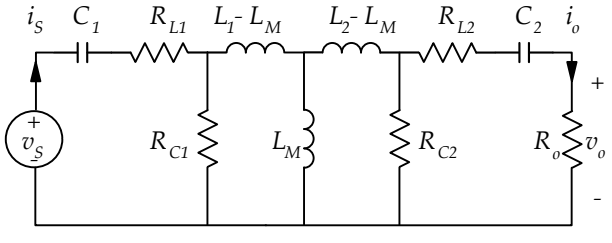

Fig. 9. Equivalent model for a coupled LC resonator including core losses.

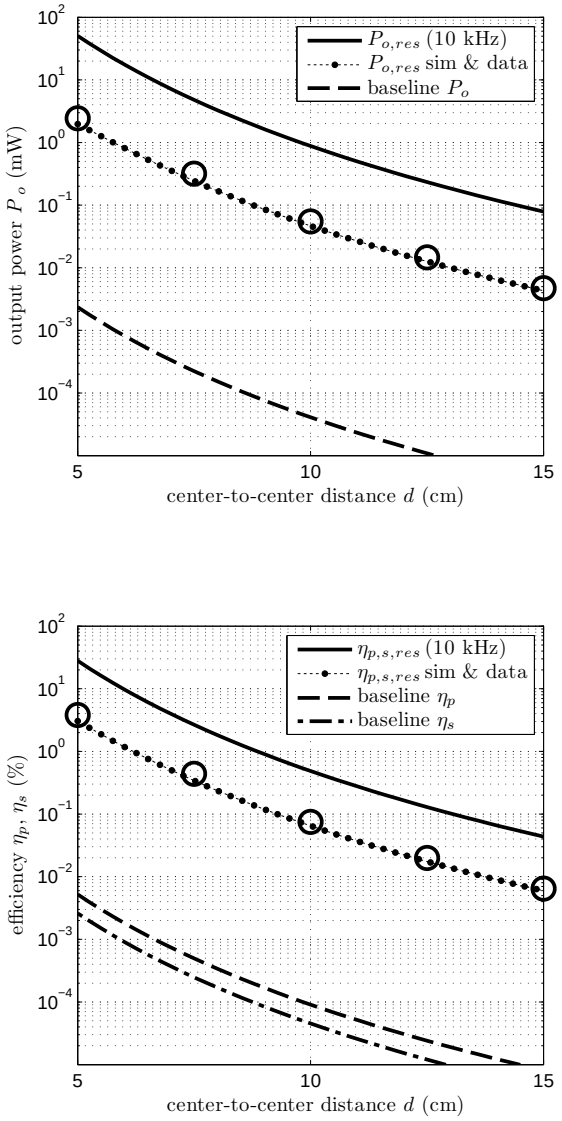

Fig. 10. Power transferred and efficiency as a function of distance for two ferrite core coils where the sender is driven with a sinusoid of amplitude $V_s = 5$ V at $f_{max,res} = 10$ kHz. Both the sender and receiver coils have an inductance of $L_1 = L_2 = 110$ mH, a series resistance of $R_{L_1} = R_{L_2} = 69\ \Omega$, a core loss resistance $R_{C_1} = R_{C_2} = 500$ kΩ, a negligible parasitic capacitance and a series capacitance $C_1 = C_2 = 2.2$ nF. The output resistance was set to $R_{o,max,res} = 69\ \Omega$. The system is bounded by the expressions derived from the resonant model and the baseline model. The data is compared to a simulation of the resonant model that includes the core losses of the coils as shown in Figure 9. The efficiencies η_p and η_s are normalized with respect to the real power and the apparent power sent by the source, respectively.

VIII. Conclusion

The LTI model shown in Figure 2 captures the behavior of weakly coupled magnetic resonators as long as the core losses and parasitic capacitance of coils can be ignored. The results indicate that, for any given coil, maximizing the resonant frequency increases the power transferred and the efficiency given the constraints imposed by the parasitics. Furthermore, the model also indicates some of the limitations of this system. In particular, as the frequency increases, so does the quality factor of the resonators. This makes the system more sensitive to errors in the relative tuning of each resonator and in the driving frequency. Furthermore, the addition of core losses and parasitic capacitances of each coil captures the degradation of the system as it is pushed to higher frequencies. Nevertheless, the model is a useful design tool at lower frequencies. The primary design limitation within this region is probably the heat dissipation within the coils which limits the maximum voltage that can be applied at the source resonator.

Combining Equation 2 and Equation 14 yields an expression that relates real efficiency $\eta_{p,res}$ to separation distance d,

$$\eta_{p,res} = \frac{Q_1 Q_2}{16(d/\sqrt{r_1 r_2})^6} \tag{21}$$

A resonator with an inductance of 16 mH and a capacitance of 160 pF will resonate at 100 kHz. If the losses in the resonator are 10 Ω, the resulting Q will be 1,000. These resonators would be able to send power a distance 9 times their radius $r = r_1 = r_2$ with an efficiency of 10%. However, the efficiency drops as $1/d^6$. This means that the efficiency at $8r$ is 25%, while the efficiency at $10r$ is 5%.

The system demonstrated in [4] had an efficiency of 30% at $7.5r$ using resonators with a Q of 1,000, and Equation 21 above predicts an efficiency of 35%. Since their maximum efficiency $\eta_{max,res} = 95\%$, the condition for weak coupling and the validity of the model given by Equation 9 is $d \gg 4.8r$.

Appendix A
Derivation of the Maximum Power Transferred Using Inductive Magnetic Coupling

The transfer function V_o/V_s for the circuit shown in Figure 3 is

$$\frac{V_o}{V_s} = \left[\frac{\kappa\sqrt{\frac{L_2}{L_1}}s}{s + \frac{R_{L_1}}{L_1} - \kappa^2 s\frac{\frac{L_2}{R_{L_2}+R_o}s}{\frac{L_2}{R_{L_2}+R_o}s+1}}\right]\left[\frac{\eta_{max,res}}{\frac{L_2}{R_{L_2}+R_o}s+1}\right], \tag{22}$$

where $\eta_{max,res}$ is defined in Equation 11. Assuming $\kappa \ll 1$,

$$\frac{V_o}{V_s} \approx \left[\kappa\sqrt{\frac{L_2}{L_1}}\cdot\frac{s}{s+\frac{R_{L_1}}{L_1}}\right]\left[\frac{\eta_{max,res}}{\frac{L_2}{R_{L_2}+R_o}s+1}\right]. \tag{23}$$

The power output at R_o is

$$\begin{aligned} P_o &= \frac{|V_s|^2}{2R_o}\left|\frac{V_o}{V_s}\right|^2 \\ &= \frac{|V_s|^2}{2R_o}\cdot\kappa^2\frac{L_2}{L_1}\cdot\frac{\eta_{max,res}^2|s|^2}{|s+\frac{R_{L_1}}{L_1}|^2|1+\frac{L_2}{R_{L_2}+R_o}s|^2}, \end{aligned} \tag{24}$$

which is maximized when

$$f_{max}(R_o) = \frac{1}{2\pi}\sqrt{\frac{R_{L_1}(R_{L_2}+R_o)}{L_1 L_2}} \tag{25}$$

and

$$R_{o,max}(f) = \sqrt{R_{L_2}^2 + (L_2\cdot 2\pi f)^2}. \tag{26}$$

The intersection of these two condition yields the optimum values for frequency and load resistance in Equations 4 and 5.

Substitution of these values into the equation for power output P_o results in Equation 6. The voltage gain at this optimum is

$$\left.\frac{V_o}{V_s}\right|_{s=j2\pi f_{max}, R_o=R_{o,max}} = \frac{\kappa}{2}\sqrt{\frac{L_2}{L_1}}. \tag{27}$$

Note that since the magnitude of the apparent power S_s has to be larger than the real power P_s, the real efficiency η_p, given in Equation 7, must also be greater than the apparent efficiency η_s given in Equation 8. In particular,

$$\eta_p = \eta_s\sqrt{2}\sqrt{1+\frac{R_{L_2}/L_2}{R_{L_1}/L_1}}. \tag{28}$$

If the sender and receiver coils are identical, $\eta_p = 2\eta_s$. Since

$$\frac{R_{L_2}/L_2}{R_{L_1}/L_1} \geq 0, \tag{29}$$

then $\eta_p \geq \sqrt{2}\eta_s$. The best case possible is $R_{L_2}/L_2 \ll R_{L_1}/L_1$, in which case $\eta_p = \sqrt{2}\eta_s$. This corresponds to the case where the real power equals the reactive power at the source. In every other case, the reactive power will be larger.

If the output resistance R_o is not equal to $R_{o,max}$, the power output is

$$\begin{aligned} P_o\Big|_{s=j2\pi f_{max}} &= \frac{|V_s|^2}{2R_o}\left|\frac{V_o}{V_s}\right|^2_{s=j2\pi f_{max}} \\ &= \frac{|V_s|^2}{2R_o}\left[\kappa\sqrt{\frac{L_2}{L_1}}\cdot\frac{R_o}{R_{L_1}\frac{L_2}{L_1}+R_{L_2}+R_o}\right]^2 \end{aligned} \tag{30}$$

and the voltage gain becomes

$$\left.\frac{V_o}{V_s}\right|_{s=j2\pi f_{max}} = \kappa\sqrt{\frac{L_2}{L_1}}\cdot\frac{R_o}{R_{L_1}\frac{L_2}{L_1}+R_{L_2}+R_o}. \tag{31}$$

These expressions are useful to measure the magnetic coupling coefficient κ using different load resistances R_o.

Appendix B
Derivation of the power transferred using magnetic resonant coupling

The circuit shown in Figure 2 shows coupled resonators connected to a source on one end and a load resistor on the other. Assuming Equation 9 is satisfied, the voltage across L_M is

$$\frac{V_{L_M}}{V_s} \approx \frac{L_M s}{1/C_1 s + L_1 s + R_{L_1}}, \tag{32}$$

which is maximum at

$$\frac{1}{2\pi}\frac{1}{\sqrt{L_1 C_1}}. \tag{33}$$

The maximum gain at this frequency is

$$\frac{V_{L_M}}{V_s} = j\kappa\sqrt{\frac{L_2}{L_1}}Q_1, \tag{34}$$

where Q_1 is defined in Equation 10. Similarly,

$$\frac{V_o}{V_{L_M}} = \frac{R_o}{1/C_2 s + (L_2 - L_M)s + R_{L_2} + R_o}, \tag{35}$$

which is maximum at

$$\frac{1}{2\pi}\frac{1}{\sqrt{(L_2-L_M)C_2}} \approx \frac{1}{2\pi}\frac{1}{\sqrt{L_2 C_2}}, \tag{36}$$

and where the gain becomes

$$\frac{V_o}{V_{L_M}} = \eta_{max,res}. \tag{37}$$

Assuming each capacitor resonates with its respective inductor at the same frequency, the overall gain is

$$\frac{V_o}{V_s} = j\kappa\sqrt{\frac{L_2}{L_1}}Q_1\eta_{max,res}. \tag{38}$$

After maximizing the voltage gain as a function of frequency, the power output at R_o is

$$\begin{aligned} P_{o,res} &= \frac{|V_s|^2}{2R_o}\left|\frac{V_o}{V_s}\right|^2 \\ &= \frac{|V_s|^2}{2R_{L_1}}\kappa^2 Q_1 Q_2 \eta_{max,res}(1-\eta_{max,res}), \end{aligned} \tag{39}$$

and the efficiency is

$$\eta_{p,res} = \kappa^2 Q_1 Q_2 \eta_{max,res}(1-\eta_{max,res}), \tag{40}$$

both of which are maximized when $\eta_{max,res} = 1/2$ and $R_{o,max,res} = R_{L_2}$. The voltage gain in this case is

$$\left.\frac{V_o}{V_s}\right|_{s=j2\pi f_{max}, R_o=R_{o,max}} = j\frac{\kappa}{2}\sqrt{\frac{L_2}{L_1}}Q_1. \tag{41}$$

and the maximum power and efficiency are given by Equations 12 and 14, respectively.

Acknowledgment

Special thanks to Professor Jeffrey H. Lang for his suggestions and guidance, and to Ashley Walker for her work on Tesla's contribution to wireless power transfer as part of her Olin Self Study degree requirement throughout the spring term of 2009.

References

[1] N. Tesla, "Apparatus for transmission of electrical energy," U.S. Patent 649,621, dated May 15, 1900.

[2] E. Waffenschmidt and T. Staring, "Limitation of inductive power transfer for consumer applications," in *13th European Conference on Power Electronics and Applications*, 2009, pp. 1–10.

[3] X. Liu, W. M. Ng, C. K. Lee, and S. Y. R. Hui, "Optimal operation of contactless transformers with resonance in secondary circuits," *IEEE*, pp. 645–650, 2008.

[4] A. Kurs, A. Karalis, R. Moffatt, J. D. Joannopoulos, P. Fisher, and M. Soljačić, "Wireless Power Transfer via Strongly Coupled Magnetic Resonances," *Science*, vol. 317, no. 5834, pp. 83–86, 2007.

[5] A. Karalis, J. Joannopoulos, and M. Soljačić, "Efficient wireless non-radiative mid-range energy transfer," *Annals of Physics*, vol. 323, no. 1, pp. 34–48, 2008.

[6] X. C. Wei, E. P. Li, Y. L. Guan, and Y. H. Chong, "Simulation and experimental comparison of different coupling mechanisms for the wireless electricity transfer," *Journal of Electromagnetic Waves and Applications*, vol. 23, no. 7, pp. 925–934, 2009.

[7] C. Zhu, C. Yu, K. Liu, and R. Ma, "Research on the topology of wireless energy transfer device," in *Vehicle Power and Propulsion Conference, 2008. VPPC '08. IEEE*, Sept. 2008, pp. 1–5.

[8] C. Zhu, K. Liu, C. Yu, R. Ma, and H. Cheng, "Simulation and experimental analysis on wireless energy transfer based on magnetic resonances," in *Vehicle Power and Propulsion Conference, 2008. VPPC '08. IEEE*, Sept. 2008, pp. 1–4.

[9] *Sony develops highly efficient wireless power transfer system based on magnetic resonance*. Sony Corporation, 2009, Sony Press Release accessed October 23, 2009. [Online]. Available: http://www.sony.net/SonyInfo/News/Press/200910/09-119E/index.html

[10] *Intel CTO Says Gap between Humans, Machines Will Close by 2050*. Intel Corporation, 2008, Intel News Release accessed October 23, 2009. [Online]. Available: http://www.intel.com/pressroom/archive/releases/20080821comp.htm

[11] D. J. Griffiths, *Introduction to Electrodynamics*, 2nd ed. Prentice-Hall: Englewood Cliffs, NJ, 1989.

[12] H. A. Haus and J. R. Melcher, *Electromagnetic Fields and Energy*. Prentice-Hall: Englewood Cliffs, NJ, 1989.